Unclassified

SECURITY CLASSIFICATION OF THIS PAGE *(When Data Entered)*

REPORT DOCUMENTATION PAGE		READ INSTRUCTIONS BEFORE COMPLETING FORM
1. REPORT NUMBER AFWAL-TR-80-3141, Part II	2. GOVT ACCESSION NO.	3. RECIPIENT'S CATALOG NUMBER
4. TITLE *(and Subtitle)* INVESTIGATION OF HIGH-ANGLE-OF-ATTACK MANEUVER-LIMITING FACTORS: PART II: Piloted Simulation Assessment of Bihrle Departure Criteria		5. TYPE OF REPORT & PERIOD COVERED Final Report 13 May 1976 - 30 July 1980 6. PERFORMING ORG. REPORT NUMBER TR-1081-1
7. AUTHOR(s) David G. Mitchell Donald E. Johnston		8. CONTRACT OR GRANT NUMBER(s) F33615-76-C-3072
9. PERFORMING ORGANIZATION NAME AND ADDRESS Systems Technology, Inc. 13766 S. Hawthorne Blvd. Hawthorne, CA 90250		10. PROGRAM ELEMENT, PROJECT, TASK AREA & WORK UNIT NUMBERS PE 62201F
11. CONTROLLING OFFICE NAME AND ADDRESS AFWAL/FIGC Air Force Wright Aeronautical Laboratories Air Force Systems Command Wright-Patterson AFB, OH 45433		12. REPORT DATE December 1980 13. NUMBER OF PAGES 51
14. MONITORING AGENCY NAME & ADDRESS *(if different from Controlling Office)*		15. SECURITY CLASS. *(of this report)* Unclassified 15a. DECLASSIFICATION/DOWNGRADING SCHEDULE

16. DISTRIBUTION STATEMENT *(of this Report)*

Approved for public release; distribution unlimited

17. DISTRIBUTION STATEMENT *(of the abstract entered in Block 20, if different from Report)*

18. SUPPLEMENTARY NOTES

19. KEY WORDS *(Continue on reverse side if necessary and identify by block number)*

High AOA
Flying Qualities
Stall/Departure
Simulation

20. ABSTRACT *(Continue on reverse side if necessary and identify by block number)*

The high-angle-of-attack, low-speed stall/departure characteristics of the F-4J and F-14A are analyzed, using a six-degree-of-freedom mathematical model with nonlinear aerodynamics. Cause-effect relationships are investigated for maneuver limiting factors including wing rock, nose slice, and rolling departures. Cross-derivatives of $\mathcal{L}_{\dot{\alpha}}$, $N_{\dot{\alpha}}$, and M_{β} alter key transfer function

(continued)

DD FORM 1 JAN 73 1473 EDITION OF 1 NOV 65 IS OBSOLETE

Unclassified

SECURITY CLASSIFICATION OF THIS PAGE *(When Data Entered)*

parameters. A piloted simulation validates analytic predictions and demonstrates that departure warning, susceptibility, and severity are strongly influenced by the static cross-derivatives. A connection between roll numerator parameter values and pilot perception of departure susceptibility and severity is identified. Potential modifications for the high AOA sections of the MIL-F-8785B Flying Qualities Specification are proposed: a criterion for the real part of the roll numerator root, further recommendations for minimizing departure susceptibility and certain sideslip influences, and a flying quality rating form for assessing departure and recovery characteristics.

Part I, Analysis and Simulation, presents a summary of the complete investigation and results. Part II, Piloted Simulation Assessment of Bihrle Departure Criteria, presents a detailed comparison of analytical prediction and piloted simulation results for a specific set of programmed control deflections. Part III, Appendices — Aerodynamic Models, contains the detailed aerodynamic models employed in the F-4J and F-14A high-angle-of-attack analysis and validation and the equations of motion, aerodynamic models, control system configurations, etc., employed in the piloted simulation.

FOREWORD

This research was sponsored by the Air Force Wright Aeronautical Laboratories, Air Force Systems Command, under Contract F33615-76-C-3072, Work Unit 24030514. Mr. Gary K. Hellmann was the initial project monitor. This responsibility was later transferred to Mr. Michael E. Bise (AFWAL/FIGC). Support of the piloted simulation was also provided by the Naval Air Development Center where Mr. Mark Stifel served as project monitor. The analytic work was performed at Systems Technology, Inc., Hawthorne, California. The work was performed during the period 13 May 1976 through 30 July 1980. The STI Technical Director was Mr. I. L. Ashkenas. Mr. D. E. Johnston was Principal Investigator and STI Project Engineer. The piloted simulation was accomplished at the McDonnell Aircraft Co., St. Louis, Missouri. The report manuscript was submitted in September 1980.

The authors wish to express acknowledgment and thanks to their many coworkers for contributions, both general and detailed, in the program: at STI, Mr. G. L. Teper for invaluable aid in accomplishing the digital simulation, Mr. T. T. Myers for development and validation of the F-4 and F-14 aerodynamic models and for most of the initial analytic support, and Mr. R. H. Hoh for checkout and accomplishment of the piloted simulation. Mr. Hoh also served as one of the subject pilots. At MCAIR, Mr. H. Passmore directed setup and operation of the piloted simulation. Special thanks are due to Lt. Col. R. M. Cooper, Maj. J. A. Fain, Jr., and Maj. J. Jannarone of the 6510th Test Wing and Maj. P. Tackabury of the Test Pilot School, Edwards Air Force Base, for their contribution in refining the high angle of attack flying quality rating scale and their professional approach in accomplishing the sometimes tedious simulation experiments.

Finally, appreciation is extended to Mr. P. Kelly of Grumman Aircraft Co. and Mr. M. Humphreys of the Naval Air Test Center for support in obtaining much of the F-14 data and information, to Mr. R. Wood of the Air Force Flight Test Center for invaluable comments and suggestions concerning the flying quality rating scale, and to Mr. R. Woodcock (AFWAL/FIGC) for his careful critique and editorial refinement of this final report.

TABLE OF CONTENTS

LIST OF ILLUSTRATIONS

LIST OF TABLES

NOMENCLATURE

AOA	Angle of attack
a_y'	Lateral acceleration at pilot's station, ft/sec^2
b	Wing span, ft
CAS	Command augmentation system
$\bar{c}$	Wing mean aerodynamic chord, ft
C_{ℓ_α}	$\partial C_{\ell_\beta} \cdot \beta / \partial \alpha$, 1/deg
C_{ℓ_β}	Effective dihedral derivative, 1/deg
$C_{\ell_{\delta_a}}$	Aileron effectiveness derivative, 1/deg
$C_{\ell_{\delta_{sp}}}$	Rolling spoiler effectiveness derivative, 1/deg
$C_{\ell_{\delta_{stk}}}$	Lateral stick effectiveness derivative, 1/in. ($C_{\ell_{\delta_{stk}}} = 8.08\ C_{\ell_{\delta_a}} + 11.58\ C_{\ell_{\delta_{sp}}}$)
C_{m_β}	$\partial C_m(\alpha,\beta)/\partial \beta$, 1/deg
C_{n_α}	$\partial C_{n_\beta} \cdot \beta / \partial \alpha$, 1/deg
C_{n_β}	Directional stability derivative, 1/deg
$C_{n_{\beta dyn}}$	$C_{n_\beta} \cos \alpha - \frac{I_z}{I_x} C_{\ell_\beta} \sin \alpha$, 1/deg
$C_{n_{\delta_a}}$	Yaw due to ailerons, 1/deg
$C_{n_{\delta_{sp}}}$	Yaw due to rolling spoilers, 1/deg
$C_{n_{\delta_{stk}}}$	$8.08\ C_{n_{\delta_a}} + 11.58\ C_{n_{\delta_{sp}}}$, 1/in.
FCS	Flight control system
g	Gravitational constant, 32.2 ft/sec^2
h	Altitude, ft
I_x, I_y, I_z	Moments of inertia about body axes, slug-ft^2
I_{xz}	Product of inertia about body axes, slug-ft^2
$\mathcal{L}_\alpha$	$\partial \mathcal{L} / \partial \alpha$, 1/sec^2
$\mathcal{L}_\beta$	$\partial \mathcal{L} / \partial \beta$, 1/sec^2
$\mathcal{L}_p$	$\partial \mathcal{L} / \partial p$, 1/sec

NOMENCLATURE (continued)

$\mathcal{L}$,M,N	Total aerodynamic moments about body axes x, y, z respectively
LCDP	Lateral control divergence parameter, $C_{n_\beta} - C_{\ell_\beta}\left(\frac{C_{n_{\delta_a}}}{C_{\ell_{\delta_a}}}\right)$
m	Aircraft mass, slugs
M	Mach number
M_β	$\partial M/\partial\beta$, $1/sec^2$
n_z	Normal acceleration, g
N_α	$\partial N/\partial_\alpha$, $1/sec^2$
N_β	$\partial N/\partial\beta$, $1/sec^2$
$N_{\delta a}$	$\partial N/\partial\delta_a$, $1/sec^2$
$N_{\delta_{DH}}$	$\partial N/\partial\delta_{DH}$, $1/sec^2$
$N^{\theta}_{\delta_{stab}}$	Numerator of the transfer functions for stabilator control of pitch attitude
p,q,r	Total inertial angular velocities about body axes, deg/sec
p_c	Roll rate command, deg/sec
PSG	Post stall gyration
$\bar{q}$	Dynamic pressure, psf
s	Laplace operator, $\sigma \pm j\omega$
S	Wing reference area, ft^2
SAS	Stability augmentation system
SRI	Stick-to-rudder interconnect
t	Time
T_{θ_3}	Time constant of first-order nonminimum phase root of $N^{\theta}_{\delta_{stab}}$ (coupled)
u,v,w	Perturbational linear velocities along the x, y, and z body axes, ft/sec
V_T	Total linear velocity, ft/sec
W	Aircraft weight, lbs
X,Y,Z	Aerodynamic forces along an axis system with x axis aligned with the total velocity vector; z axis in aircraft plane of symmetry pointing down; and y axis orthogonal to x and z axes and positive out right wing

NOMENCLATURE (concluded)

Z_w	Total external force due to aerodynamics, thrust, and gravity acting along the z axis
α	Angle of attack, deg
$\hat{\alpha}$	Peak α prior to control neutralization, Bihrle criteria
β	Sideslip angle, deg
δ_a	Aileron surface deflection, deg
δ_{stk}	Lateral stick deflection, $(8.08\,\delta_a + 11.58\,\delta_{sp})$, in.
δ_r	Rudder surface deflection, deg
δ_{sp}	Rolling spoiler surface deflection, deg
δ_{stab}	Horizontal stabilator surface deflection, deg
τ	Time constant of SRI lag
φ,θ,ψ	Euler angles between gravity-oriented inertial axis and aircraft body axis, deg
ω	Total angular velocity, $\sqrt{p^2 + q^2 + r^2}$, ft/sec
ω_φ	Natural frequency of complex $N^{\varphi}_{\delta_{stk}}$ root
ω_d	Natural frequency of dutch roll

SECTION I

INTRODUCTION

The principal goals and accomplishments of this research program are documented in Part I, "Analysis and Simulation" (Ref. 1). Part II documents a portion of the piloted simulation and data analysis performed at the request of the U. S. Navy, Naval Air Development Center, which provided a portion of the simulation funds. The NADC desired that the high AOA, open-loop, full-control-deflection, departure-inducing maneuver employed in Ref. 2 be performed in a piloted simulation. The object was to determine if results are comparable to those obtained in purely digital computation (simulation) runs and to obtain pilot assessment of the maneuver's validity in evaluating airframe departure susceptibility. In addition, the departure susceptibility of the simulated aerodynamic configurations was predicted using the analytic criterion of Ref. 2 and compared with similar predictions based upon the closed-loop criterion of Ref. 3.

For a number of years, a principal concern of the fighter aircraft industry has been design for high AOA departure resistance. Departure is defined (Ref. 4) as:

> "... the event in the post-stall flight regime which precipitates entry into a post-stall gyration, spin, or deep-stall condition. The departure may be characterized by divergent, large-amplitude, uncommanded aircraft motions, such as nose-slice or pitch-up. Departure is synonymous with complete loss of control."

However, pilots generally place a rate threshold on the uncommanded motion. Rates below the threshold are interpreted as natural warning that a limit is being (has been) reached, that the pilot must back off to regain positive control. If the aircraft returns to controlled flight the aircraft is considered departure resistant. Rates above the threshold raise the distinct problem of the pilot not being able to prevent the uncommanded motion

from continuing. If this is the case (e.g., after a slight delay in neutralizing controls), the aircraft is considered departure-susceptible. The aircraft is considered extremely susceptible if departure generally occurs with the normal application of pitch control alone, or with small roll and yaw control inputs (Ref. 4).

Thus, departure susceptibility involves two aspects: open-loop static and dynamic stability, and pilot/vehicle closed-loop stability. The first is relatively straightforward to predict or demonstrate, including the influences of steady aggravated control inputs. The second is not, since it may be dependent upon pilot technique or skill.

This volume presents a review of the aerodynamic parameters shown in Part I to dominate high AOA dynamic characteristics; a brief description of two criteria currently being proposed or utilized for analytical prediction of high AOA departure susceptibility; and results of two series of simulations applied to evaluate these criteria. The simulations consisted of: first, a fully digital, unpiloted, computer analysis (described in Part III); and, second, a piloted simulation (described in Parts I and III).

A. KEY HIGH AOA PARAMETERS

The key aerodynamic derivatives shown in the Ref. 1 analysis to dominate aircraft open-loop departure warning, susceptibility, and severity are summarized in Table 1. On the left are the key open-loop parameters; on the right are the maneuver-limiting dynamic characteristics associated with the open-loop parameter. Negative $N_{\delta a}$ or $N_{\delta D}$ (differential stabilator) is a causal factor of roll reversal. This information is nothing new; the effect has been observed on a number of aircraft. Adverse "aileron" yaw is a key parameter in that it signifies the onset of large sideslip excursions in maneuvering flight. The second open-loop parameter identified is M_β, pitching moment due to sideslip. Positive M_β results in pitch-up with sideslip; negative, pitch-down. The remaining static coupling and cross-coupling derivatives (and the one damping derivative) all contribute to wing rock, nose slice, and roll divergence characteristics. A given aircraft response depends upon the relative values of these six coefficients. One can get any

or all of these motions, depending upon the coefficient values and ratios. The importance of $\mathcal{L}_\beta$, N_β, and L_p is widely recognized. In the vicinity of stall, aerodynamic moments generally become highly nonlinear functions of both α and β and the cross-coupling derivatives $\mathcal{L}_\alpha$, N_α, and M_β can become quite large at $\beta \neq 0$.

The Vol. I analysis also identified key closed-loop departure parameters (Table 2). These are associated with the numerator factors (roots) for the vehicle over which active piloted control is being exerted.

TABLE 1. KEY OPEN-LOOP DEPARTURE PARAMETERS

Negative N_{δ_a} or $N_{\delta_{DH}}$	Roll Reversal
Positive M_β	Pitch Up
$\mathcal{L}_\beta, \mathcal{L}_\alpha, \mathcal{L}_p$ N_β, N_α M_β	Wing Rock Nose Slice Roll Divergence

TABLE 2. KEY CLOSED-LOOP DEPARTURE PARAMETERS

Aileron Maneuvering Control	$\frac{\omega_\varphi^2}{\omega_d^2} \sim \frac{LCDP}{C_{n_{\beta_{dyn}}}}$	Roll Reversal Wing Rock Roll Departure
	$1/T_\varphi$	Nose Slice
Rudder or Aileron Maneuvering Control	$\frac{1}{T_s^\theta}$	Nose Slice

For aileron-only maneuvering control a key parameter is the ratio of ω_φ^2 to ω_d^2. The ratio is proportional to LCDP/$C_{n_{\beta_{dyn}}}$ (as shown in Refs. 3 and 5), which at zero sideslip derives from the nondimensional forms of the aerodynamic coefficients of Table 1:

$$\frac{\text{LCDP}}{C_{n_{\beta_{dyn}}}} = \frac{C_{n_\beta}\left[1 - \dfrac{C_{n_{\delta_a}} C_{\ell_\beta}}{C_{\ell_{\delta_a}} C_{n_\beta}}\right]}{C_{n_\beta} \cos\alpha - \dfrac{I_z}{I_x} C_{\ell_\beta} \sin\alpha}$$

Undesirable ratios lead to open- or closed-loop troubles such as roll reversal, pilot-aggravated wing rock (PIO), and roll departure. In the presence of sideslip, the expressions become complicated by additional terms involving C_{ℓ_α}, C_{n_α}, C_{m_β}, and trig functions of β.

Two additional closed-loop departure parameters for either rudder or aileron maneuvering control are identified in Table 2. However, these have no bearing on the airframe open-loop departure characteristics of interest in this volume, and will not be further discussed.

B. CONFIGURATIONS AND PREDICTED HIGH AOA CHARACTERISTICS

Table 3 summarizes the six-configuration matrix employed in the overall program. The configurations are identified on the left; in the center are the aerodynamic terms varied; and on the right are anticipated high AOA characteristics, based upon analysis and open-loop time responses. Configuration A has the aerodynamics of the basic F-4J aircraft; A_1 is an unaugmented airframe and A_2 has lateral/directional augmentation added (see Part III, Appendix I). For A_1 a sequence of wing rock, roll reversal, nose slice, and finally rolling departure is predicted with increasing AOA. For A_2 the augmentation system and a lateral stick-to-rudder cross-feed are expected to minimize or eliminate the roll reversal and wing rock departure warnings. Thus, the predicted characteristics are nose slice, followed by rolling departure. For B, the aerodynamic roll damping parameter, C_{ℓ_p}, was increased. This aero configuration was used only with the

TABLE 3. CONFIGURATION MATRIX

CONFIGURATION	FCS	AERO VARIANT	PREDICTED CHARACTERISTICS
A_1	Basic	Basic F-4J	Wing rock Roll reversal Nose slice Roll depart
A_2	Aug		Nose slice Roll depart
B	Basic	Increased C_{ℓ_p}	Roll reversal Nose slice Roll depart
C_1	Basic	Increased C_{ℓ_β} $15 < \alpha < 45$ Decreased C_{ℓ_α}	Wing rock Roll reversal Roll depart
C_2	Aug		$C_{n_{\beta_{dyn}}} > 0$ None LCDP > 0
D	Basic	Increased C_{n_β} $\alpha > 15$ Decreased C_{n_α} Positive C_{m_β}	Wing rock Roll reversal Pitch-up

basic manual control system in order to compare the high AOA stall/departure characteristics of an aircraft with naturally high roll damping (Configuration B) with that obtained with artificially augmented roll damping (Configuration A_2). For B, predicted departure characteristics are roll reversal, nose slice, and rolling departure. With the large roll damping of this configuration wing rock should not be present. For C, the rolling moment coefficient as a function of α and β was modified in the AOA range between 15 and 45 deg to approximate that of the F-14A aircraft. The unaugmented Configuration C_1 is predicted to exhibit wing rock, roll reversal, and rolling divergence with increasing AOA but no nose slice. An augmented flight control system was also employed with C to determine if it would improve or degrade the departure characteristics of this configuration. The airframe and flight control characteristics were selected so that $C_{n_{\beta dyn}}$ and LCDP are both greater than zero throughout the usable AOA range for the configuration. On the basis of these parameters, no departure tendency would be anticipated for this configuration. Finally, D employed altered static yawing moment characteristics for AOA greater than 15 deg to increase C_{n_β} and decrease C_{n_α}. The end result is an airframe mildly directionally unstable at AOA greater than 25 deg, which should exhibit wing rock and roll reversal warnings. A second modification incorporated in D was a change in sign of C_{m_β} to provide positive pitching moment with sideslip. This should result in pitchup, which would be expected to aggravate any high AOA departure characteristics. All other configurations had negative C_{m_β}. For the investigation of the Bihrle criterion, only the unaugmented configurations are employed, since the criterion was derived on that basis.

SECTION II

PREDICTION CRITERIA

The susceptibility to, and severity of, departure may be predicted via the Weissman departure/spin criterion (Ref. 3) as well as the more recent Bihrle criterion (Ref. 2). Both of these are based upon static aerodynamic coefficients.

A. WEISSMAN CRITERION

The Weissman criterion, Ref. 3, is a plot of $C_{n_{\beta dyn}}$ vs. LCDP divided into four regions of increasing departure and spin susceptibility and severity (Fig. 1). This criterion was employed in selecting the static aerodynamic coefficients which determined vehicle Configurations A through D. The criterion predicts high departure/spin susceptibility with strong rolling departures for configurations A_1 and B, which are identical here since C_{ℓ_p} has no influence on either parameter; moderate susceptibility and rolling departures for Configuration C_1; and no departure for Configuration D. Thus, all regions of departure susceptibility and severity are exercised with the aerodynamics selected.

B. BIHRLE CRITERION

The Bihrle criterion (Ref. 2) relates roll reversal and departure susceptibility to the raw static aerodynamic coefficients $C_{n_{\delta a}}$, C_{n_β}, and C_{ℓ_β}. Figure 2 presents the boundaries for an aircraft exhibiting adverse $C_{n_{\delta a}}$. Two boundaries are included. The upper, dashed boundary is the roll reversal criterion. Above the dashed line no roll reversal is predicted; below the dashed line the aircraft should exhibit roll reversal. The lower solid boundary is the departure criterion. Again, above the boundary there is no departure; below the boundary the criterion predicts a departure.

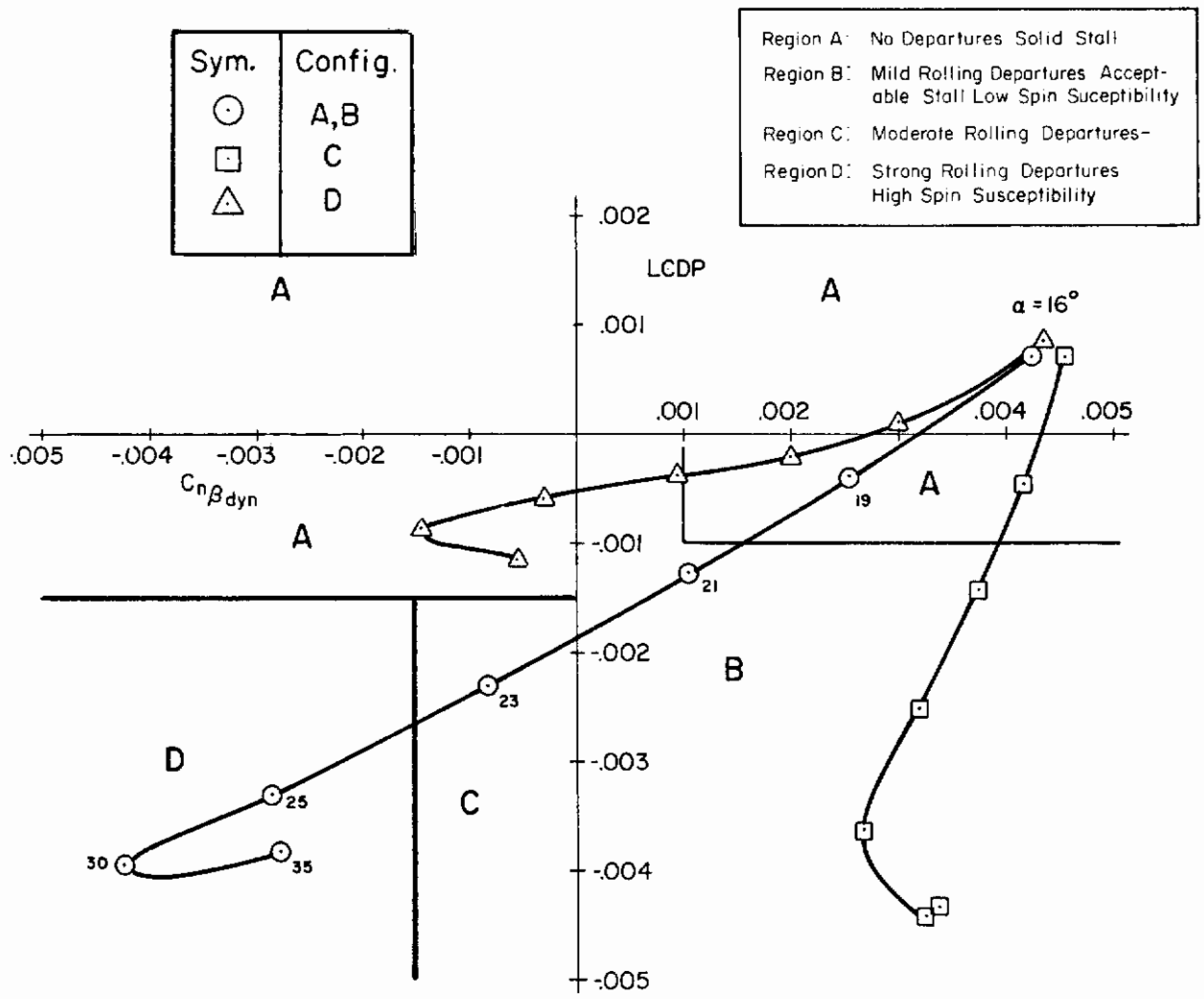

Figure 1. Weissman Criterion Predictions

The interpretation is that the Bihrle criterion predicts, for the Aircraft Cases A and B, roll reversal above about 10 deg AOA. At approximately 20 deg AOA the region is entered in which departure might be expected. Out to 30 deg AOA, C_{ℓ_β} is small while C_{n_β} is large and negative, so that one would expect a strong directional divergence or nose slice characteristic. At yet higher angles of attack, C_{ℓ_β} increases negatively while C_{n_β} decreases in magnitude; so one might expect more of a rolling divergence characteristic.

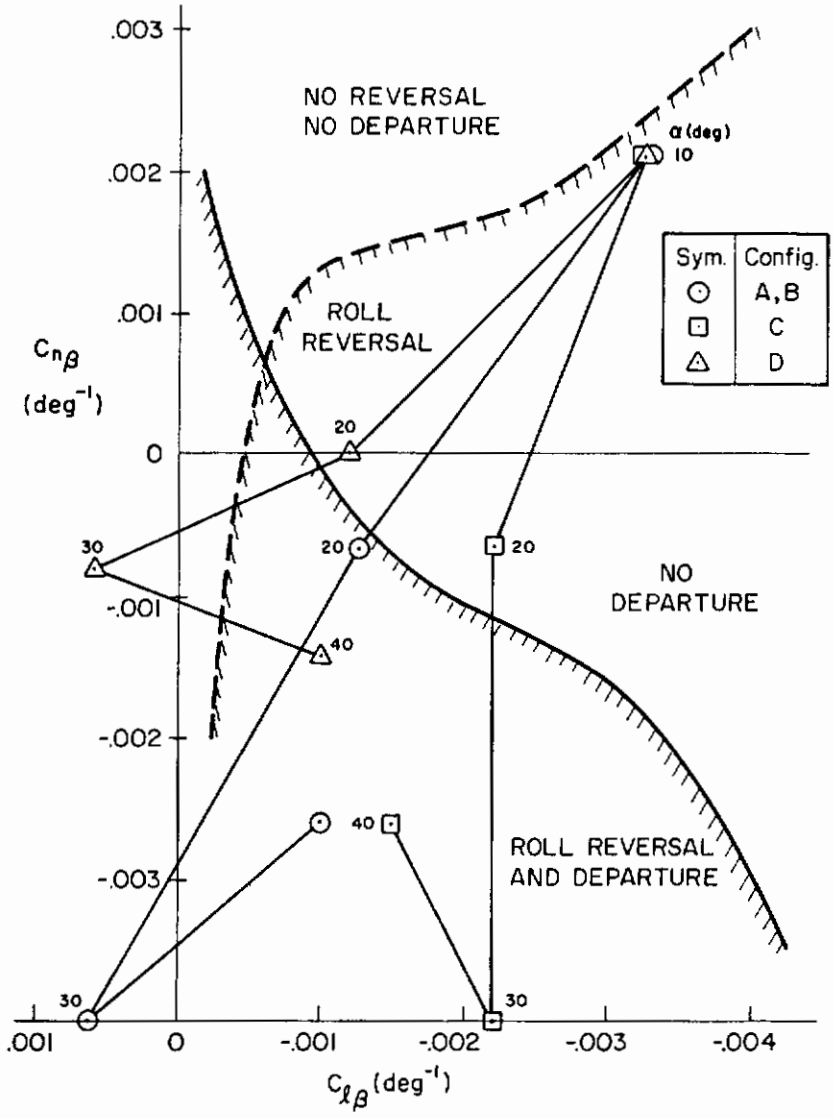

Figure 2. Bihrle Criterion Predictions
(Adverse $C_{n_{\delta_a}}$)

Configuration C, on the other hand, stays somewhat closer to the departure criterion boundary and is well to the right of the roll reversal boundary. Therefore, the criterion predicts this configuration to exhibit significant adverse yaw, roll due to sideslip, and, above 20 deg AOA, rolling departure.

Configuration D stays closer to both of the criterion boundaries. It therefore lies in a gray area because a slight shift in either of the criterion boundaries could change predictions regarding both roll reversal and departure tendencies. The interpretation is that Configuration D should have mild, if any, roll reversal characteristics and mild, if any, rolling departure characteristics.

There is considerable similarity between the AOA loci plots of Figs. 1 and 2. This is because LCDP $\doteq C_{n_\beta}$ when C_{ℓ_β} and $C_{n_{\delta_a}}$ are small and $C_{n_{\beta_{dyn}}} \sim C_{\ell_\beta}$ when $C_{n_\beta} << C_{\ell_\beta}$. Thus, one should expect the two criteria to be substantially in agreement in the region of interest, i.e., where static or dynamic stability is critically low. The Bihrle criterion, however, is the simpler of the two and therefore may be easier to apply in the midst of wind tunnel testing.

In summary, the four vehicle configurations selected are predicted to exhibit a broad spectrum of high AOA departure warning, susceptibility, and severity characteristics for assessment by the pilots.

SECTION III

BIHRLE MANEUVER

The Ref. 2 departure/roll reversal susceptibility boundaries were established from responses of a digital simulation model of an aircraft to a "canned" full-control-deflection maneuver. The airplane was trimmed in a 60 deg bank angle turn at 35,000 ft altitude and Mach 0.9. The control inputs were then applied:

- t = 0, full trailing-edge up longitudinal control applied at a rate of 30 deg/sec
- t = 1.5 sec, full lateral control applied at 30 deg/sec to oppose the turn
- t = 8 sec, both controls returned to trim at a rate of 30 deg/sec
- Rudder remained undeflected

The last AOA peak magnitude ($\hat{\alpha}$) prior to control removal was related to departure indication. 50 deg (10 deg above maximum AOA trim) was chosen as an indication of departure susceptibility. Similarly, studies of peak bank angle at the time lateral control was removed led to the boundaries for uncoordinated roll reversals. Reference 2 did not contain time response traces, which would have helped in assessing the severity and/or type of aircraft motions involved.

The aerodynamic configurations developed for this key maneuver-limiting factor investigation fell within the bounds of the Ref. 2 aero envelopes, and the vehicle mass and inertia characteristics are similar (see Table 4). Therefore, nonlinear 6 DOF computer runs of the maneuvers were made prior to the piloted simulation in order to check the criterion validity and the severity of resulting motion for our configurations. The principal deviation between the two investigations is that our vehicles were trimmed to the 60 deg bank angle at 15,000 ft altitude, 0.46 Mach, α_o = 12 deg and departure is defined as $\hat{\alpha} > 47$ deg (10 deg above maximum trim), whereas Bihrle used 35,000 ft altitude, 0.9 Mach, with departure defined as $\hat{\alpha} > 50$ deg. Our control inputs were identical to those used in Ref. 2; however

TABLE 4. AIRCRAFT MASS AND INERTIA CHARACTERISTICS

	Ref. 2 (Inertial Model B)	CASES A_1, B, C_1, D
b, ft	40	38.67
$\bar{c}$, ft	10	16.04
S, ft^2	400	530.00
W, lbs	33,000	37,000.00
I_x, slug-ft^2	25,000	23,850.00
I_y, slug-ft^2	135,000	127,400.00
I_z, slug-ft^2	155,000	146,000.00
I_{xz}, slug-ft^2	-0-	2,210.00

Ref. 2 assumed essentially constant control surface effectiveness over the AOA range of interest. For this study lateral control effectiveness decreased with increasing AOA, starting at α = 30 deg.

Time histories of resulting motions were recorded for 12 sec. To facilitate interpretation of the motions, computer-generated images were produced from the Euler angles θ, φ, and ψ at one-second intervals. Example traces and images are presented for Configurations A_1, B, C_1, and D, in Figs. 3 through 6, respectively. All rates and accelerations are referenced to a body fixed aircraft centerline oriented axis system.

Three configurations were prone to rapid, violent motions. Configurations A_1 and B behaved quite similarly, indicating that aerodynamic roll rate damping has little influence in departure and post stall gyrations (PSG). In both cases the aircraft initially followed the lateral stick command, but then reversed. Excursions in α and β were relatively mild until roll reversal became pronounced. Yaw rate and sideslip then increased rapidly (nose slice), and the aircraft pitched down and rolled inverted in opposition to the stick command. The large sideslip produced a fast roll rate which, with the large yaw rate, produced a large positive pitch rate due to

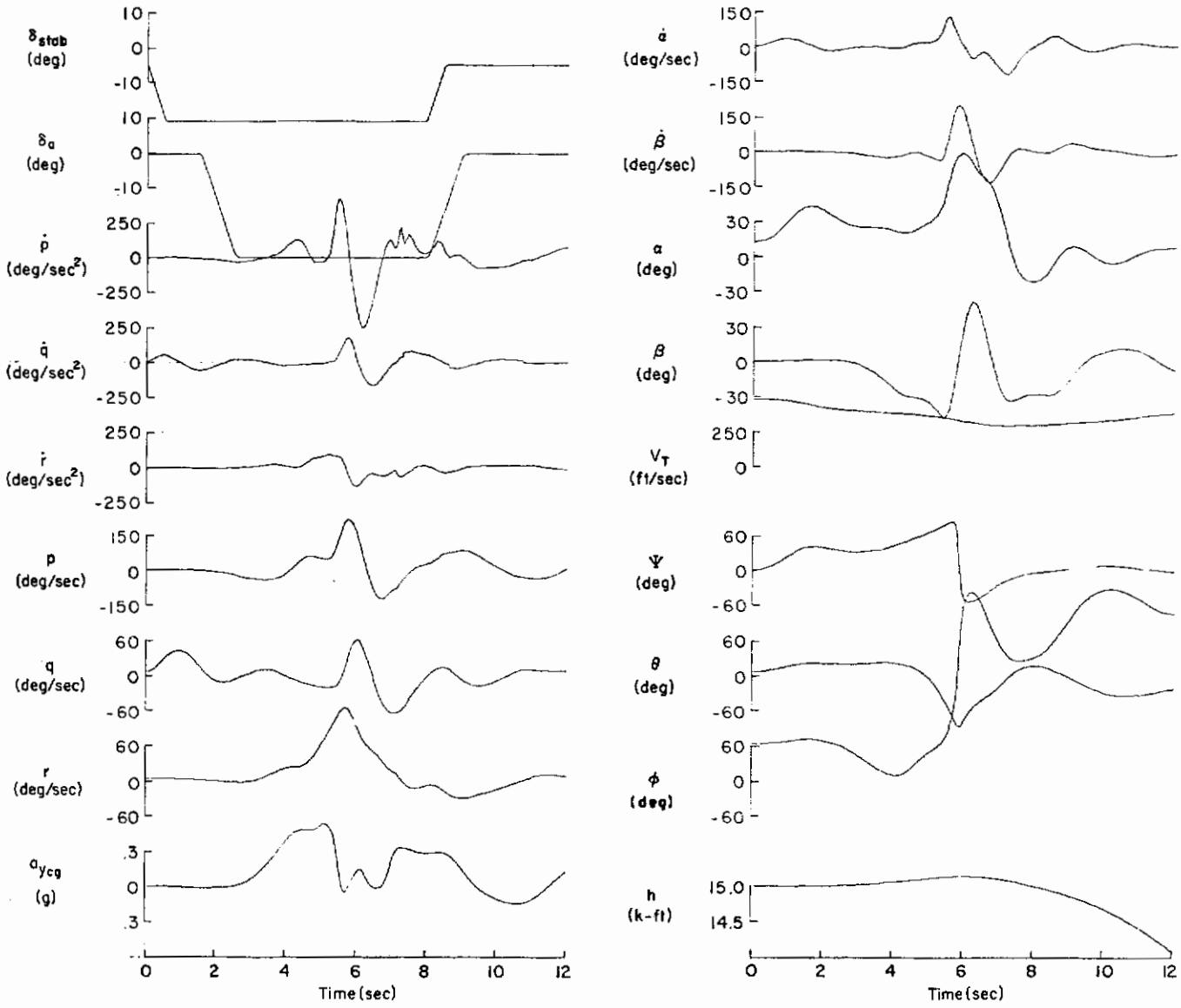

a) Time history

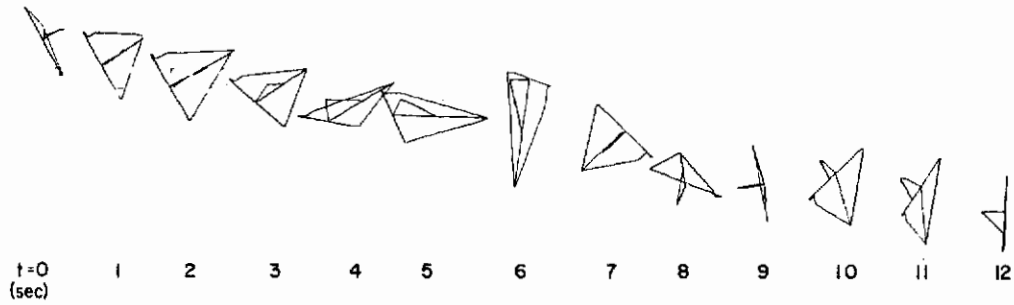

b) Aircraft images

Figure 3. Time Histories of Aircraft Response to Full-Control Maneuver; Configuration A_1

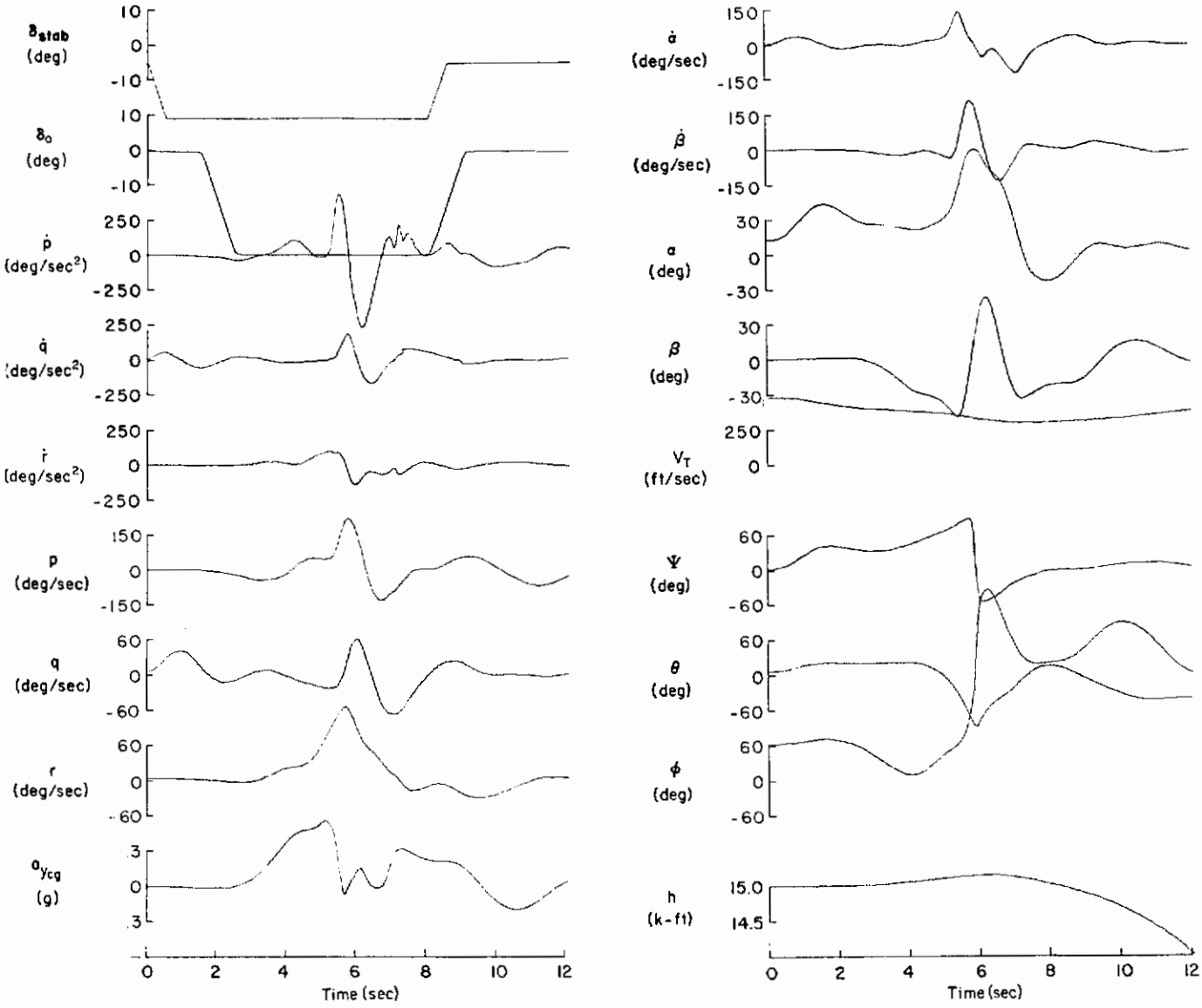

Figure 4. Time Histories of Aircraft Response to Full-Control Maneuver; Configuration B

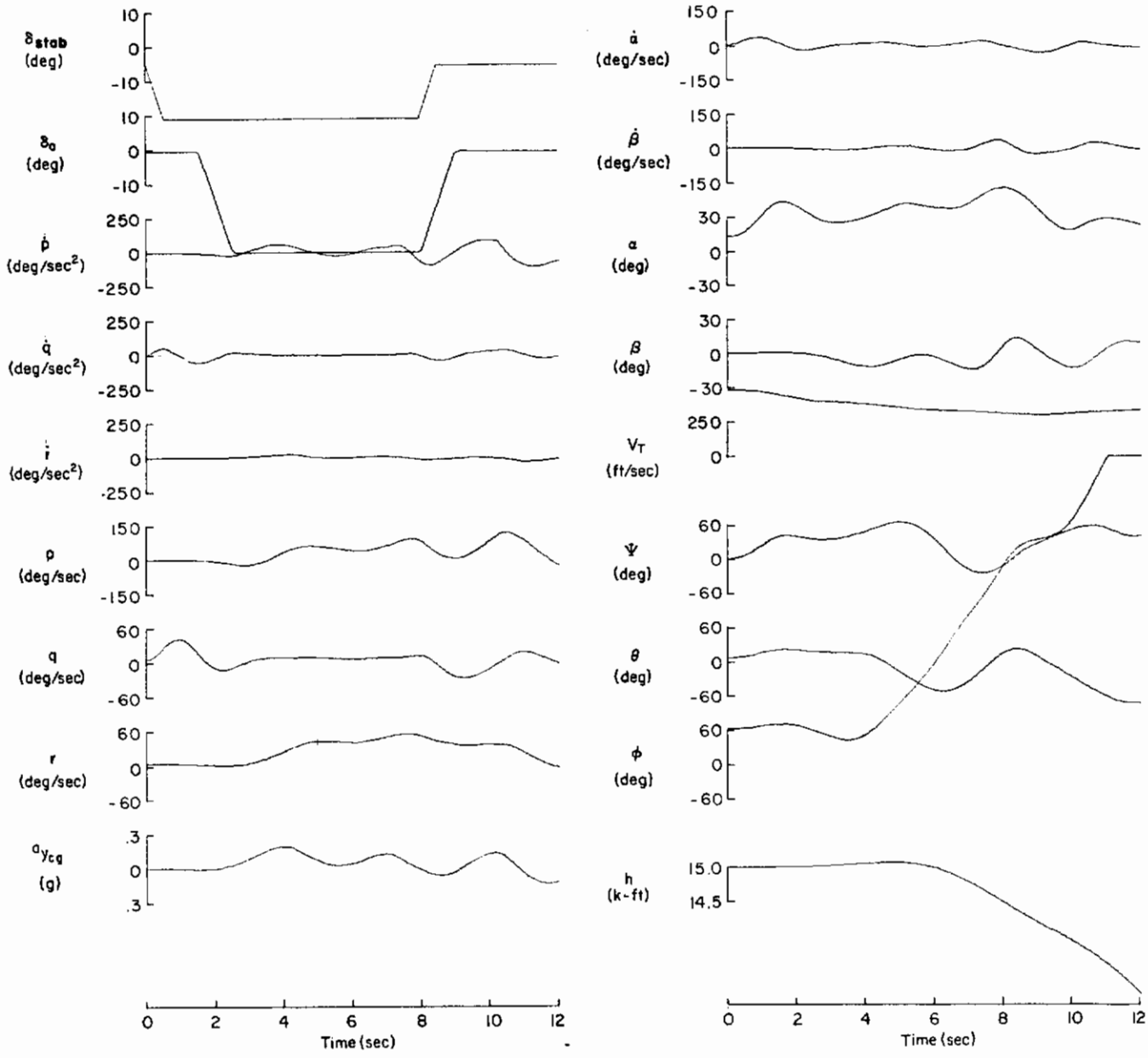

a) Time history

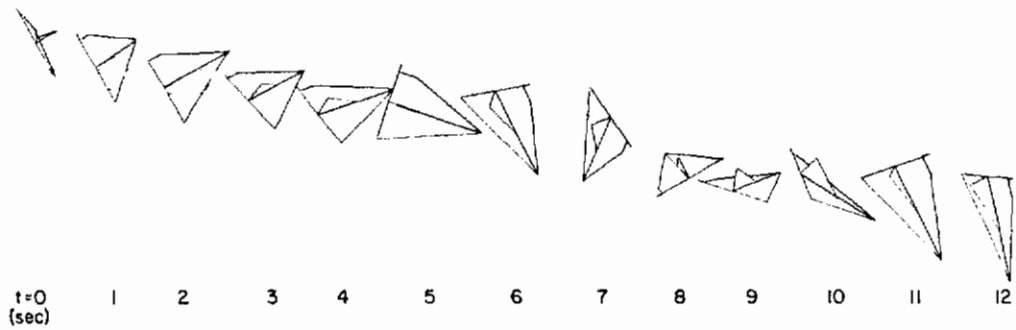

b) Aircraft images

Figure 5. Time Histories of Aircraft Response to Full-Control Maneuver; Configuration C_1

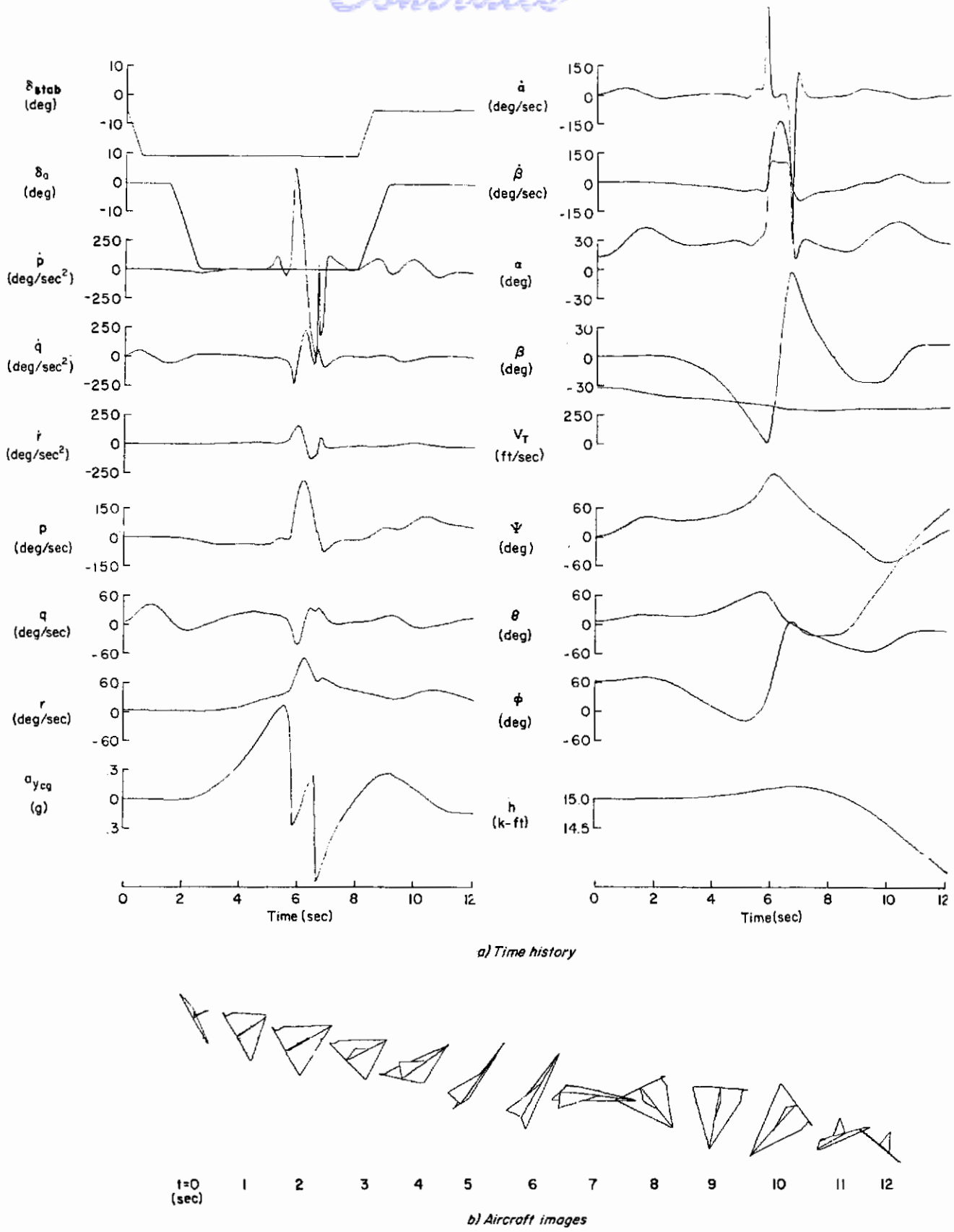

Figure 6. Time Histories of Aircraft Response to Full-Control Maneuver; Configuration D

inertial cross-coupling. This caused the large increase in AOA. The strong PSG persisted until yaw rate and/or pitch rate reduced to near zero. Following neutralization of control the aircraft rapidly settled into a 90 deg bank diving turn to the left. Both of these configurations "departed" on the basis of the Ref. 2 definition of departure, since the last α peak before neutralizing controls exceeded 47 deg (actually $\hat{\alpha} \doteq 85$ deg). Again, this peak value actually is associated with the inertia-coupled PSG.

Configuration C_1 initially followed the lateral stick command, but adverse yaw and the higher C_{ℓ_β} produced a more rapid onset of roll reversal. Pitch rate remained small so that inertia-coupled roll PSG did not occur. The aircraft made one roll about the velocity vector as it continued to roll after controls were neutralized. Based upon strict adherence to the definition of last α peak prior to control removal ($\hat{\alpha} = 40$ deg at $t = 5.2$ sec), this did not depart, although AOA was about 53 deg at the time control neutralization was initiated and the roll opposite to the command input persisted through 360 deg. (The Ref. 2 analysis did not consider roll reversal as departure. This also is consistent with Ref. 4, which requires the roll reversal to precipitate PSG, nose slice, or pitch-up, as in Configurations A_1 and B, to be considered a departure.)

Configuration D underwent the most severe motions. This was partially due to pitch-up with sideslip, but more importantly to inadequacy of the $\dot{\alpha}$ equation which was defined as:

$$\dot{\alpha} = q - \tan\beta\,(p\cos\alpha + r\sin\alpha) + Z_w/(mV_T\cos\beta)$$

Obviously this expression leads to discontinuity where $\beta = 90$ deg. Possibly because of divergence associated with the sideslip-induced pitch-up, sideslip continued to build to 90 deg for this configuration. Thus vehicle motion following the discontinuity had to be considered invalid. Even so, the aircraft recovered quite rapidly upon neutralization of controls. Overall, the motions of Configuration D were similar to those of A_1 and B prior to the PSG, except the aircraft pitched up instead of down

and sideslip built to a larger magnitude. Comparison of the yaw rate and pitch rate traces for these configurations indicates D might not be subject to inertia-coupling PSG if it were not for the $\dot{\alpha}$ equation discontinuity.

Table 5 summarizes these results of the digital simulation and compares them with predictions based upon interpretation of Fig. 2. The single definite discrepancy is with the Configuration C departure results; they depend upon which AOA peak is selected, and rejection of the continued roll reversal as a roll departure. However, these results suggest that the Ref. 2 peak AOA departure definition might be quite sensitive to inertia-coupling influences, therefore changes in vehicle inertia and/or assumed roll control power might very well result in a shifting of the boundaries of Fig. 2. The results for Configuration D also indicate the necessity for having equations of motion valid through 90 deg AOA and sideslip in dynamic analysis of post stall gyrations.

TABLE 5. BIHRLE ROLL REVERSAL/
DEPARTURE CRITERION
(Digital Simulation)

CONFIGU-RATION	REVERSAL		DEPARTURE	
	PREDICTION	OBTAINED	PREDICTED	OBTAINED
A_1	Mild	Mild	Depart	Nose slice and PSG
B	Mild	Mild	Depart	Nose slice and PSG
C_1	Strong	Strong	Depart	None
D	Mild/none	Mild	Depart	Nose slice and ?

SECTION IV

PILOTED SIMULATION

A. SIMULATION

The piloted simulation was performed at the McDonnell Aircraft Company in the 20 ft hemispherical fixed base dome identified as MACS-1. Physical aspects of the simulation are summarized in Table 6 and Fig. 7. The horizon and target are projected on the inside of the hemisphere. The cockpit is located at the center of the dome. The out-the-window, head-up, and head-down displays and cockpit layout are as indicated in Table 6. Seat cues consist of normal acceleration and buffet motion provided through an inflatable seat bladder. A TV projection of a gimballed model provides a realistic maneuvering tracking task. Two Air Force flight test pilots, experienced in high angle-of-attack departure and spin testing, served as the subject pilots.

TABLE 6. FEATURES OF PILOTED SIMULATION

FIXED BASE	McDonnell MACS-1 20 ft Dome
DISPLAYS	Horizon - 360 deg φ, θ, ψ
	HUD - CAS, h, ψ, velocity vector
	HDD - φ, θ, ψ, α, M, etc.
	Sight - Fixed reticle
COCKPIT	Basic F-4
SEAT CUES	N_z, buffet
TARGET	Gimballed model TV projection
PILOTS	2 - USAF Flight Test Center

The aerodynamic and flight control system models are described in detail in Part III (Ref. 6). The 6 DOF aerodynamic model consisted of nonlinear coefficients as a function of α and β which were stored in the digital computer as "look-up" tables. To prevent modeling discontinuities for the extreme maneuvers expected in departure and PSG, aero data

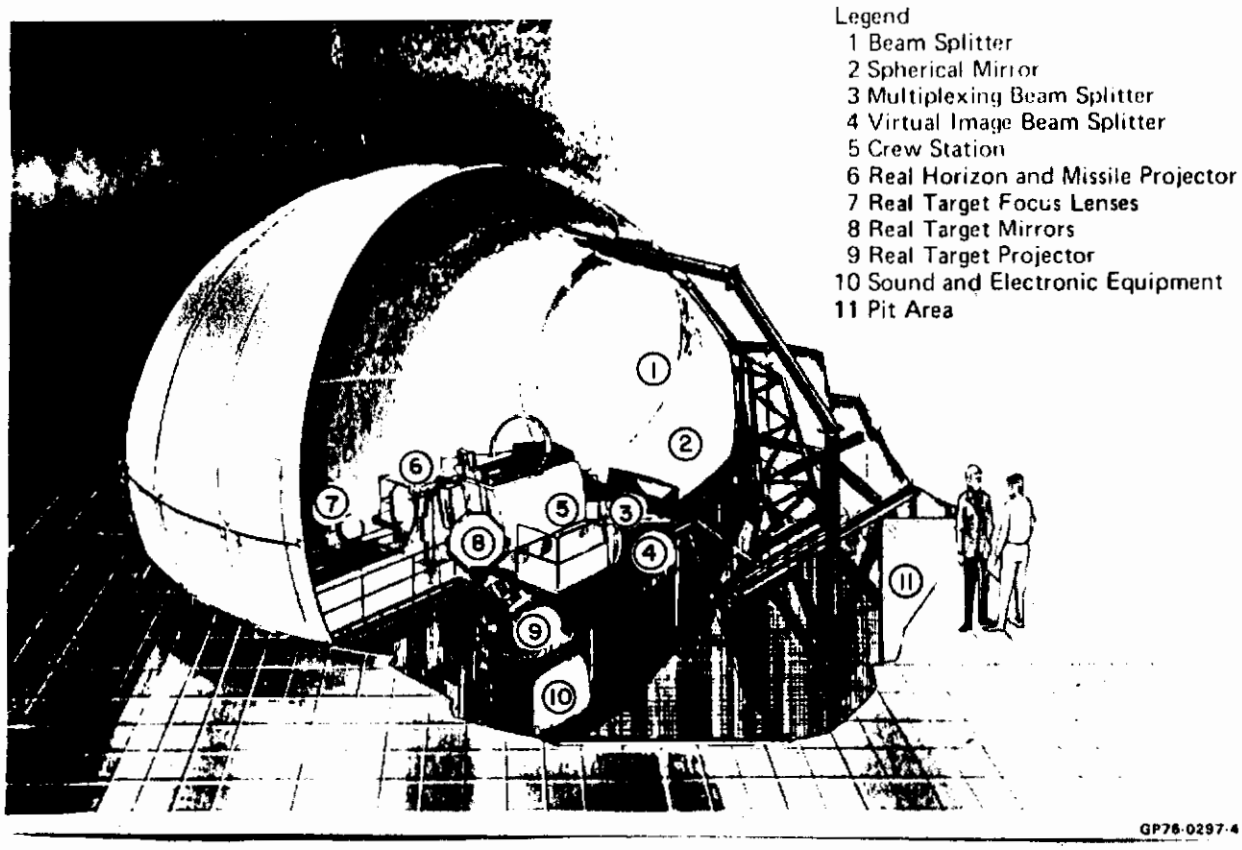

Figure 7. Manned Air Combat Simulator I

were continuous over the range $\alpha = \pm 180$ deg and $\beta = \pm 90$ deg. However, the coefficients for Configuration A_1 only reflected F-4J wind tunnel data for α between 0 and +45 deg and β up to ± 30 deg. Beyond these limits the data were extrapolated and faired to prevent discontinuities. The other three configurations were obtained by altering specific coefficient "look-up" tables as noted previously. The flight control system employed in this portion of the simulation represented the basic, unaugmented, F-4J.

Equations of motion were altered from those used in the unpiloted simulation in order to eliminate the tan β and cos β problems which occur as β approaches 90 deg with the $\dot{\alpha}$ equation. This involved substituting the $\dot{w}$ equation for $\dot{\alpha}$, i.e.,

$$\dot{\alpha} = q - \tan\beta\,(p\cos\alpha + r\sin\alpha) + Z_w/(mV_T\cos\alpha)$$
$$\dot{w} = qV_T\cos\beta - V_T\sin\beta\,(p\cos\alpha + r\sin\alpha) + Z_w/m$$

and using simple expressions, $\alpha = \sin^{-1}(w/V_T)$ and $\beta = \sin^{-1}(v/V_T)$ for entry into the aerodynamic coefficient "look-up" tables. Vehicle dynamic characteristics and responses were validated against the previous unpiloted simulation results as a check and to insure that the discontinuity noted in Fig. 6 had been eliminated.

It should be noted that the basic purpose of the piloted simulation was to validate the dominant influence of key aerodynamic coefficients on departure susceptibility, warning, and motion severity in realistic situations such as 1 g stalls and tracking maneuvering targets. Thus the aero data and equations are valid for onset of departure and PSG, but are not necessarily valid for fully developed spins or extended PSG. The full-control deflection Bihrle maneuver was employed at the request of the NADC to determine if results would agree with digital computation runs and to obtain pilot assessment of results (i.e., are pilot perceptions of departure consistent with AOA peaks of, say, 47 or 50 deg?).

B. FULL-CONTROL DEFLECTION RESULTS

Each pilot was briefed on the application of controls for the maneuver. It was stressed that control activity just prior to full-aft stick should be minimized, so that angular rates, sideslip, etc., would be small, and that rudder should not be used. The pilots counted out the timing of control inputs and flew until a well-timed maneuver was achieved.

Time histories of representative runs are shown in Figs. 8 through 11. The acceleration n_z is measured at the center of gravity, while a_y' is referenced to the pilot's station. The angular velocity ω represents the magnitude of a total angular velocity vector:

$$\omega = \sqrt{p^2 + q^2 + r^2}$$

Figure 8 shows that Configuration A_1 immediately went into a nose-high nose-slice out of the initial turn. This was followed by large amplitude pitch and roll oscillations while turning in the direction of lateral stick deflection. The large, nearly steady yaw rate and increasing AOA built toward a flat spin which was broken by early application of forward stick. The peak AOA is 60 deg at the time of forward stick. All three angular acceleration traces indicate sharp peaks caused by inertia cross-coupling during this severe departure. The inertia-coupled PSG persists long after the application of forward stick. These motions, overall, bear no resemblance to the unpiloted run of Fig. 3.

Figure 9 presents motion traces for Configuration B. The very rapid longitudinal input resulted in an AOA of about 50 deg by the time the lateral input was made. In this run the lateral stick deflection was exceptionally clean, but above 45 deg AOA lateral roll control effectiveness was small, and no roll or yaw was initiated. The basic directional instability slowly built into a nose slice to the right. The large yaw rate prior to application of forward stick, together with the resulting large pitch rate, started an inertia-coupled PSG. The last AOA peak prior to controls release was 37 deg, which is less than the departure criterion value. The departure was initiated by recovery control application. Again the motions bear no resemblance to the unpiloted run of Fig. 4.

The time traces for Configuration C_1 are shown in Fig. 10. A fairly clean lateral input was obtained, but non-ideal initial conditions apparently triggered a significant yaw acceleration prior to full lateral stick deflection. The aircraft then performed a nose slice over the top (out of the turn) and continued a 360 deg nose-low roll. It settled into a steep spiral after control release. This configuration departed, whereas the unpiloted simulation exhibited only a slow steady roll reversal with little yaw or sideslip.

Figure 11 shows the responses for Configuration D. The pilot did not get a clean lateral stick input. The inadvertent right stick started a left yaw rate and positive sideslip. However, the AOA settled out at

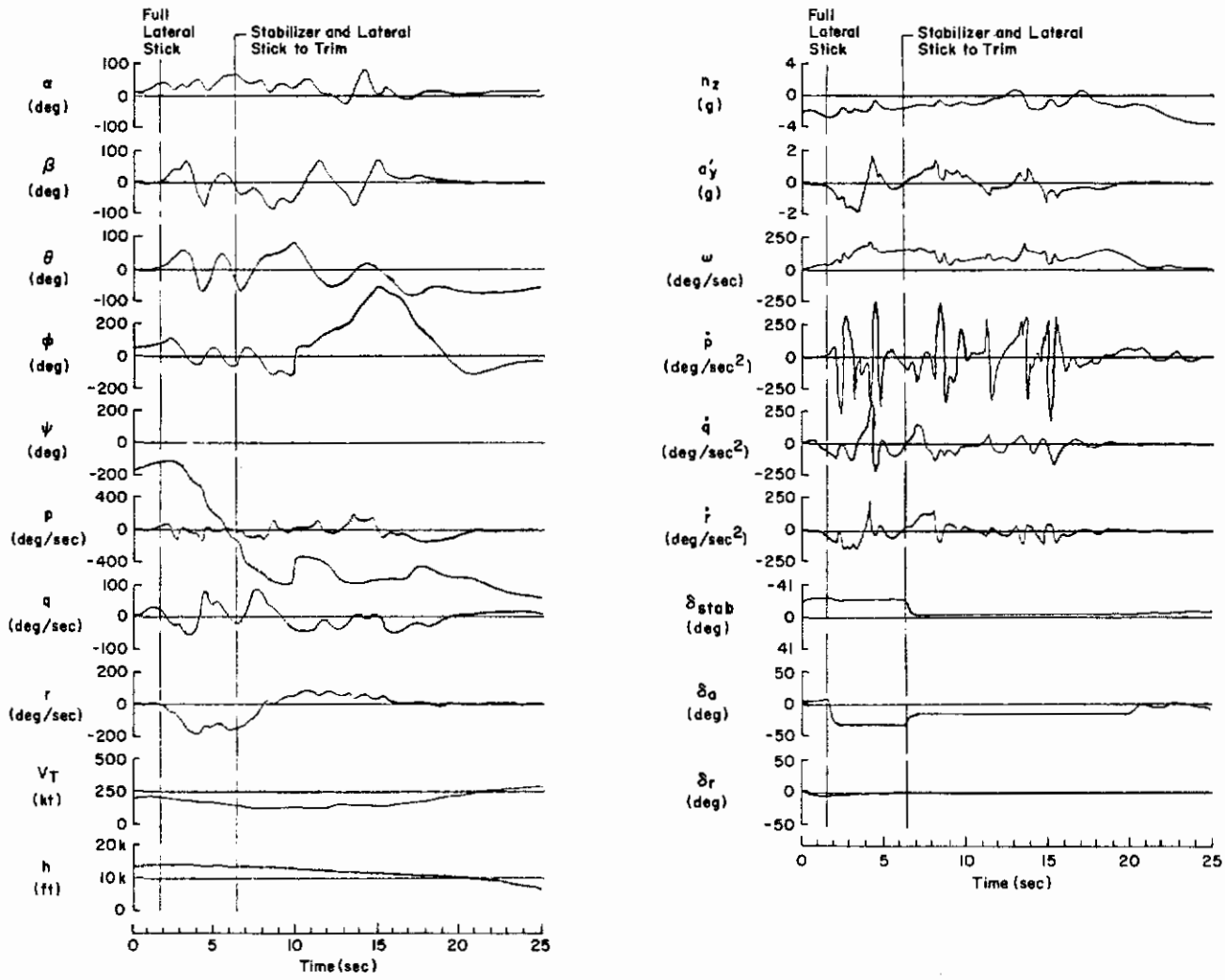

Figure 8. Response to Full-Control Maneuver (Piloted Simulation); Configuration A_1

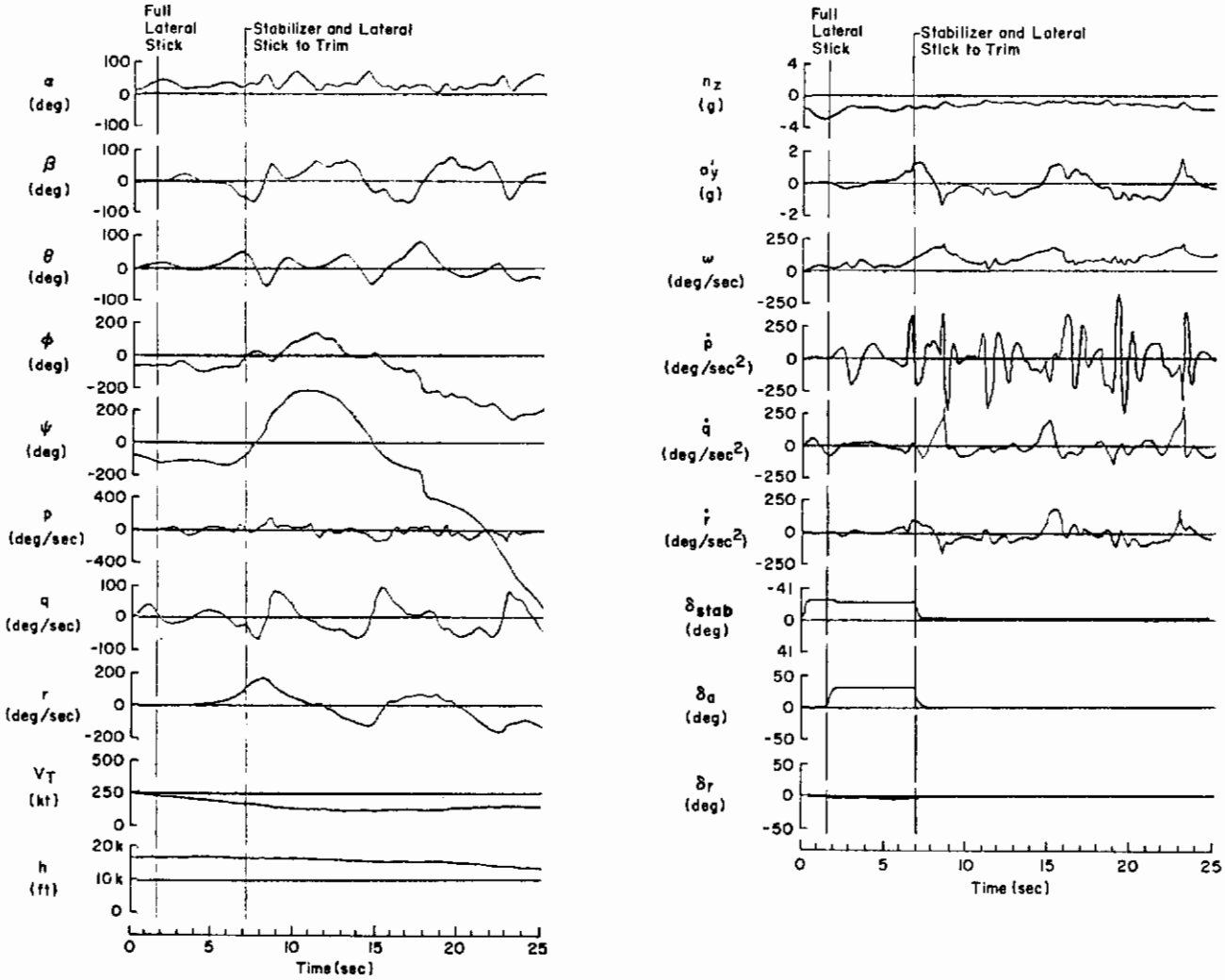

Figure 9. Response to Full-Control Maneuver (Piloted Simulation); Configuration B

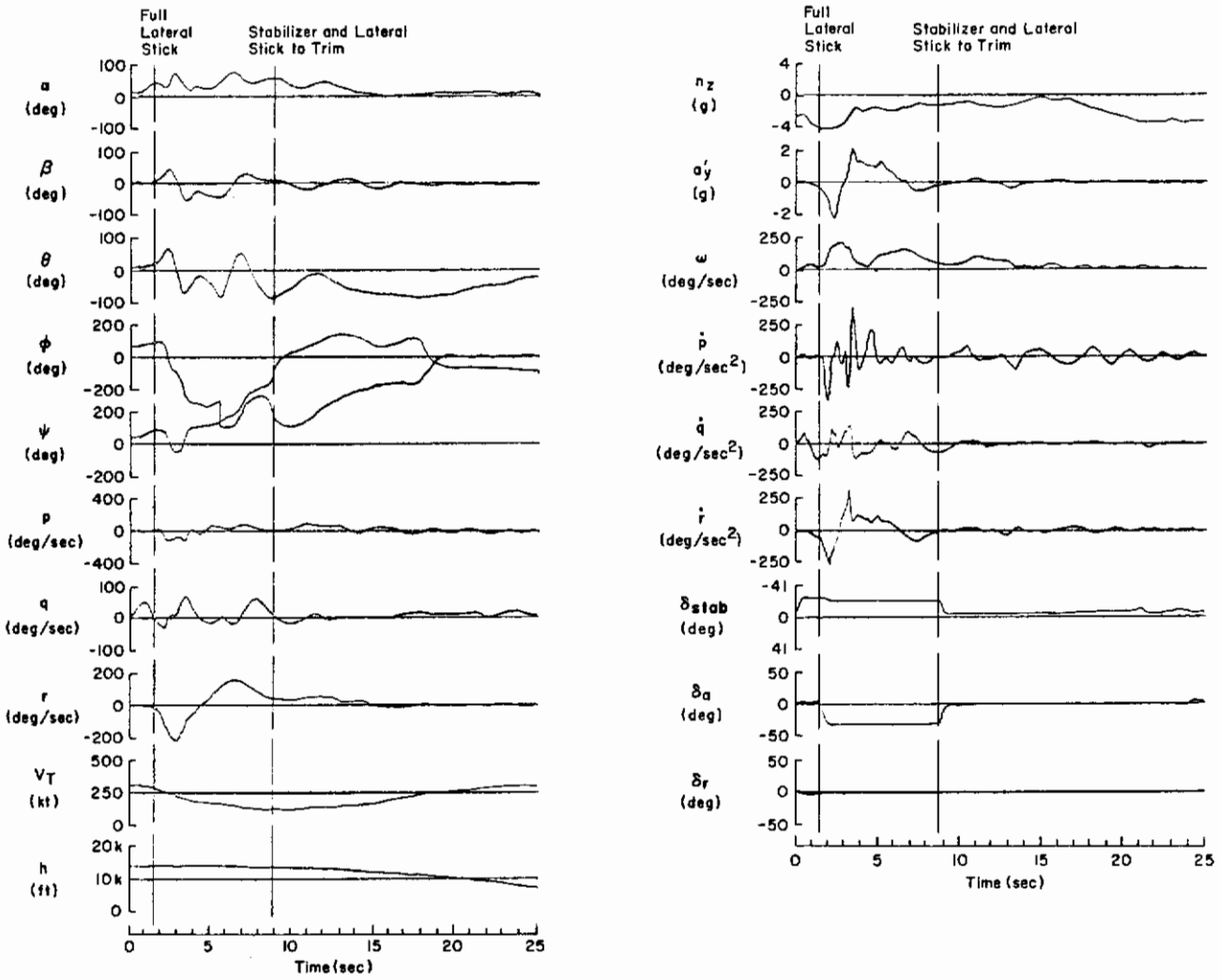

Figure 10. Response to Full-Control Maneuver (Piloted Simulation); Configuration C_1

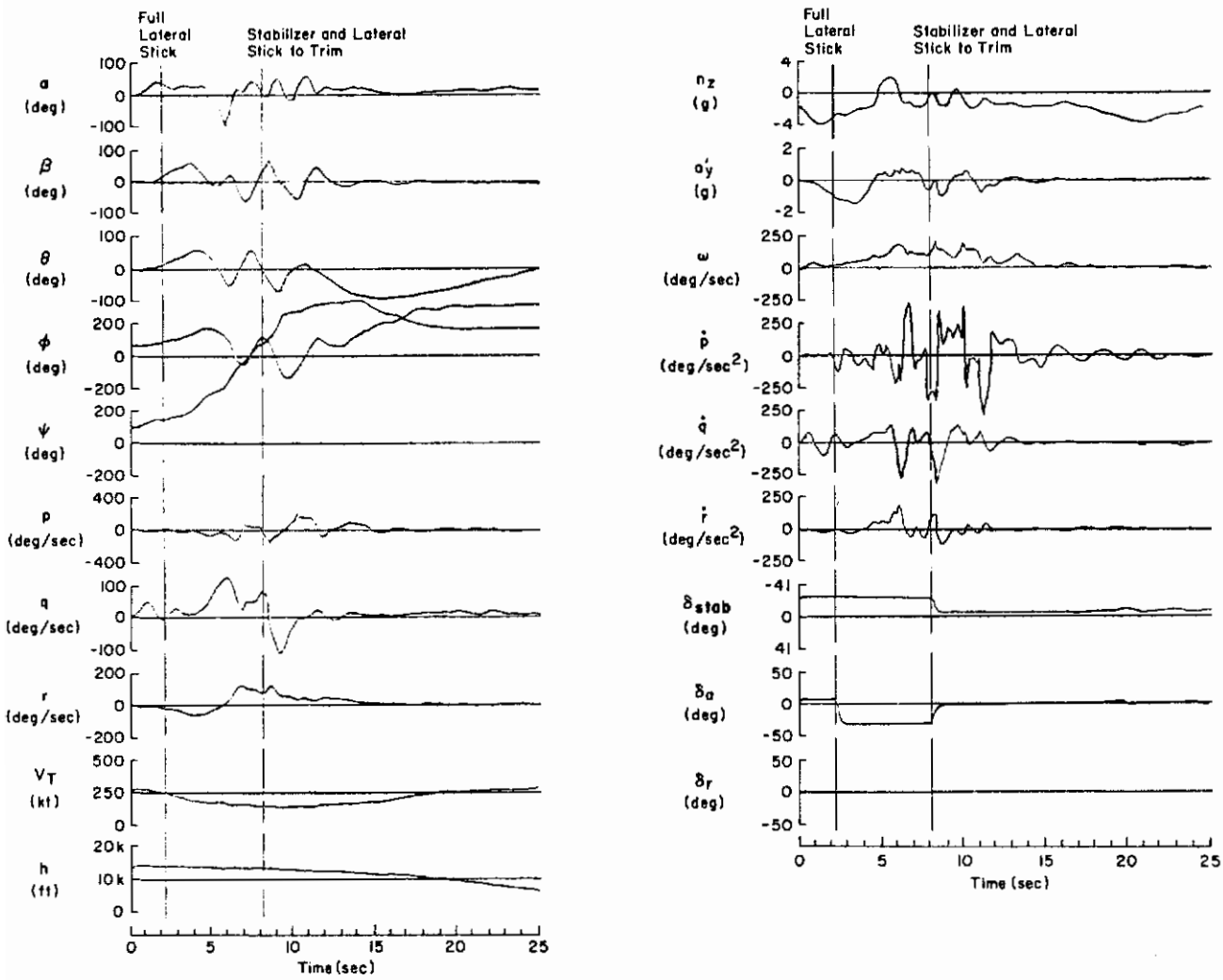

Figure 11. Response to Full-Control Maneuver (Piloted Simulation); Configuration D

about 30-35 deg where α'_β was near zero. The aircraft responded to the full aft stick and performed what amounted to an inverted stall prior to entering a PSG. Again, results were completely different from the unpiloted runs of Fig. 6.

Peak AOAs achieved prior to control neutralization in the piloted vs. unpiloted simulations are summarized in Table 7. Significant differences were obtained for all configurations.

TABLE 7. LAST ALPHA PEAK PRIOR TO CONTROL REMOVAL

CONFIGURATION	PILOTED SIMULATION	UNPILOTED SIMULATION
A_1	60	85
B	36	85
C_1	58	40
D	44	N.A.

Review of the control deflections for these runs illustrates the practical problems encountered in applying the full-control maneuver in a realistic situation:

a) Initial conditions. It was impossible for the pilots to achieve a true steady state with zero sideslip at the desired attitude and speed prior to initiating the maneuver. There always was some off-nominal condition.

b) Timing. It was difficult to apply the lateral control at precisely 1.5 sec, and to remove lateral and longitudinal controls at 8 sec. The latter time was not considered to be as important as the former because lateral control effectiveness decreased as AOA increased and therefore a delay in lateral control input resulted in less rolling acceleration.

c) Rate of application. Control application tended to be at rates higher than 30 deg/sec. This was not considered to be critical to the results, except as noted above.

d) Control fade. With full aft stick applied, application of full lateral stick resulted in a slight easing of the longitudinal control. The fade amounted to a decrease in horizontal stabilator deflection of around 2 deg.

e) Inadvertent rudder deflection. The lateral force required to deflect the control stick often resulted in some bracing against, and slight motion of, the rudder pedals. The runs shown in Figs. 8 through 11 show δ_r deflections which are uncharacteristically small.

f) Inadvertent lateral stick deflection. In almost every run some lateral stick deflection occurred in obtaining full longitudinal deflection. Figure 9 shows the cleanest such input for all the runs made. Lateral stick deflections resulted in an initial 2 to 10 deg aileron deflection into the turn.

g) Control removal. In some instances, controls were not returned to trim at the termination of the maneuver. The δ_a trace in Fig. 8 illustrates one instance. Since the Ref. 2 criteria were based on magnitudes prior to control removal, this would have no effect on the results.

Overall aircraft motion for all four cases was quite different from that obtained in the unpiloted simulation. Since the maneuver started at relatively low AOA (12 deg), all aircraft followed the initial, inadvertent lateral stick command into the turn. As AOA increased, the adverse aileron yaw created an initial yaw rate and sideslip out of the turn. Due to the rapid longitudinal stick pull, the AOA was high enough when the intentional lateral stick deflection was made that lateral surface effectiveness was very low. Thus, the aircraft motion was dominated by the initial sideslip (generally opposite to that obtained in the unpiloted simulation) and basic high AOA directional instability.

C. CRITERIA ASSESSMENT

The pilots rated departure susceptibility of each configuration on the basis of tracking a target in three maneuvers: straight-ahead climb, maneuvering climb, and wind-up turn. The bank-to-bank and wind-up turn tracking task maneuvers were similar to those recently developed for flight test evaluation of flying qualities (Refs. 7 and 8). Table 8

TABLE 8. DEPARTURE SUSCEPTIBILITY ASSESSMENT BASED ON TRACKING TASKS

DEPARTURE SUSCEPTIBILITY		
CONFIG.	PILOT	
	RC	JF
A_1	R	ES
B	S	ES
C_1	S	S-ES
D	R	R

presents departure susceptibility ratings given by each pilot using (supposedly) the definitions of resistant (R), susceptible (S), and extremely susceptible (ES) from Ref. 4. However, analysis of recorded pilot commentary and motion strip charts, supported by additional closed-loop analysis, showed that the pilots were using widely differing tracking and control techniques and rating criteria.

Pilot RC was cautious and sensitive to onset of instability. He observed all of the departure onset warnings available and adjusted his gains to follow the decreasing roll control stability boundary until he considered path control was no longer possible. Then he initiated recovery controls (stick forward, aileron and rudder neutral) and observed the resulting aircraft response. He rated the configuration on the basis of clarity of warning prior to departure.

Pilot JF was much more aggressive in acquiring and tracking the target aircraft. He set his roll control gain for stable tracking at low AOA and did not change it as he rapidly pulled into the higher AOA region. Thus he suddenly crossed the stability boundary and departed. This pilot observed no warnings whatsoever due to rapid transition through the warning region and penetration into the instability region. As a result he experienced PSGs of varying severity. Consequently his ratings were of spin susceptibility, rather than departure susceptibility.

The end result is that, in addition to the influence of static aerodynamics, the two ratings covered departure and spin susceptibility and slow vs. accelerated departure entry. Based on the Table 8 pilot assessments, it may be concluded that the configurations provided the following characteristics in departures from tracking tasks:

A_1 - adequate warning for pilot to prevent departure; but accelerated entry produces motion so rapid as to cause nonrecoverable spin

B - inadequate warning for pilot to detect departure onset; accelerated entry produces motion so rapid as to cause nonrecoverable spin

C - inadequate warning for pilot to detect departure onset; accelerated entry produces recoverable spin

D - adequate warning for pilot to prevent departure; accelerated entry will not produce spin

Finally, it should be noted that the tracking task itself can provide cues to — or conversely, mask — the onset of departure.

1. Bihrle Criterion

Table 9 presents a summary of results for both the Bihrle Criterion/ maneuver and the tracking tasks. The Fig. 2 criterion correctly predicts departure in terms of PSG for all four configurations. However the peak AOA criterion (transient peak more than 10 deg above maximum AOA) is not satisfied in two cases. Since the full-control-deflection maneuver tended to produce an accelerated spin entry, it might be expected that results as observed by the pilots should compare well with pilot JF's spin susceptibility ratings from the tracking tasks — and they do. The agreement is not quite so good in the case of pilot RC's tracking task induced departure susceptibility ratings. Pilot assessment of the vehicle motions (based on both out-the-windscreen and instrument panel displays) were not in very good agreement with the Fig. 2 criterion predictions.

TABLE 9. FULL-CONTROL DEFLECTION MANEUVER VS. TRACKING TASK DEPARTURE SUSCEPTIBILITY

CONFIGURATION	BIHRLE MANEUVER				TRACKING TASK	
	FIG. 2 CRITERION	PILOTED TRACES		COMMENTARY	RC	JF
	PREDICT	$\hat{\alpha}$	PSG	SPIN	DEPART	SPIN
A_1	Depart	Depart	Yes	50%	R	ES
B	Depart	Not	Yes	50%	S	ES
C_1	Depart	Depart	Yes	50%	S	S
D	Depart	Not	Yes	0%	R	R

TABLE 10. COMPARISON OF WEISSMAN PREDICTED AND ACTUAL DEPARTURE/SPIN SUSCEPTIBILITY RATINGS

DEPARTURE/SPIN SUSCEPTIBILITY			
CONFIG.	PRED.	RC	JF
A_1	ES	R	[ES]
B	ES	[S]	[ES]
C_1	S	[S]	[S-ES]
D	R	[R]	[R]

2. Weissman Criterion

A comparison between departure/spin susceptibility predicted by the Weissman criterion and the tracking ratings provided by the two pilots is shown in Table 10. Ratings substantially in agreement with prediction are shown in boxes. Obviously the aggressive pilot (JF) observed the worst possible characteristics of each unaugmented configuration as predicted by the criterion. The less aggressive pilot (RC) experienced something quite different for Configurations A_1 and B. Again, this pilot was primarily rating departure warning and onset. He therefore initiated recovery at lower AOA and did not experience the same spin characteristics as JF.

Overall, these results show excellent agreement regarding spin susceptibility. One important difference between prediction and simulation was the nature of departure. Figure 1 predicts predominantly rolling departure with no indication of yaw departure. Our Configurations A_1, B, and D exhibited initial yaw excursions sometimes followed by roll. Configuration C_1 exhibited three different departure modes (see Ref. 1) which were dependent upon control application at onset of departure. However, a rolling motion did predominate. Thus, the Weissman criterion left something to be desired in identifying the nature of departure observed by the pilots.

D. SUMMARY

A piloted, fixed-base simulation assessment of the full-control deflection maneuver utilized in establishing the high AOA departure criterion boundaries of Ref. 2 was performed to determine if results would agree with unpiloted (programmed input) simulation and to obtain pilot assessment of maneuver validity in evaluating airframe departure susceptibility.

Piloted versus unpiloted results did not compare well. Non-steady and off-nominal initial conditions prior to full-control-deflection inputs have a strong influence on vehicle motion. Our pilots had considerable difficulty matching the pure (non cross-coupled) surface deflections used in the digital computation runs. The resulting early disturbances, together with mistimed surface deflections, produced considerable variability from run to run. Often the piloted simulating results have little resemblance to the unpiloted runs.

Motions observed from the piloted and unpiloted simulation strip chart traces regarding PSG and spin were in agreement with the Fig. 2 criterion prediction. However, pilot assessments of the vehicle motions were not in good agreement with criterion predictions. Usefulness of the maneuver in assessing departure susceptibility was questioned because the entry is so sudden that there is no opportunity to assess any warning or departure resistance tendencies that may exist.

On the other hand, pilot assessment of airframe spin susceptibility via the Bihrle maneuver was in fairly good agreement with tracking task results. Thus it appears the maneuver may hold promise as a spin susceptibility criterion.

SECTION V

INERTIAL COUPLING INFLUENCES

During the piloted simulation assessment of the full-control deflection maneuver, it became apparent that inertial cross-coupling moments might be dominating vehicle motion. In particular, it appeared that the large excursions in AOA might be caused by inertia-coupled pitching accelerations. Therefore, for a few runs, inertia- and aerodynamic-induced pitch acceleration contributions were generated and recorded separately along with the total acceleration (see Fig. 12). These traces clearly demonstrate that for Configuration D a large negative inertial component dominates at 6 and 8 sec after the control inputs. This reduces positive AOA excursions which are building at about 7 and 9 sec, respectively. It was previously noted in conjunction with Figs. 3 and 4 that AOA increased due to inertial pitch-up for Configurations A_1 and B. This is also apparent in Figs. 8 and 9. Further, coupling appears to dominate roll acceleration traces as well in Figs. 8 through 11. Table 11 presents a summary of times when coupling appears to start and stop in traces of both the unpiloted and piloted runs.

TABLE 11. SUMMARY OF INERTIA COUPLING

	CASE	INERTIA COUPLING	
		BEGINS	ENDS
UNPILOTED SIMULATION	A_1	5.5 sec	8.0 sec
	B	5.5 sec	8.0 sec
	C_1	-	-
	D	5.5 sec	7.5 sec
PILOTED SIMULATION	A_1	3.0 sec	16.0 sec
	B	7.0 sec	>25.0 sec
	C_1	2.0 sec	7.0 sec
	D	5.5 sec	11.0 sec

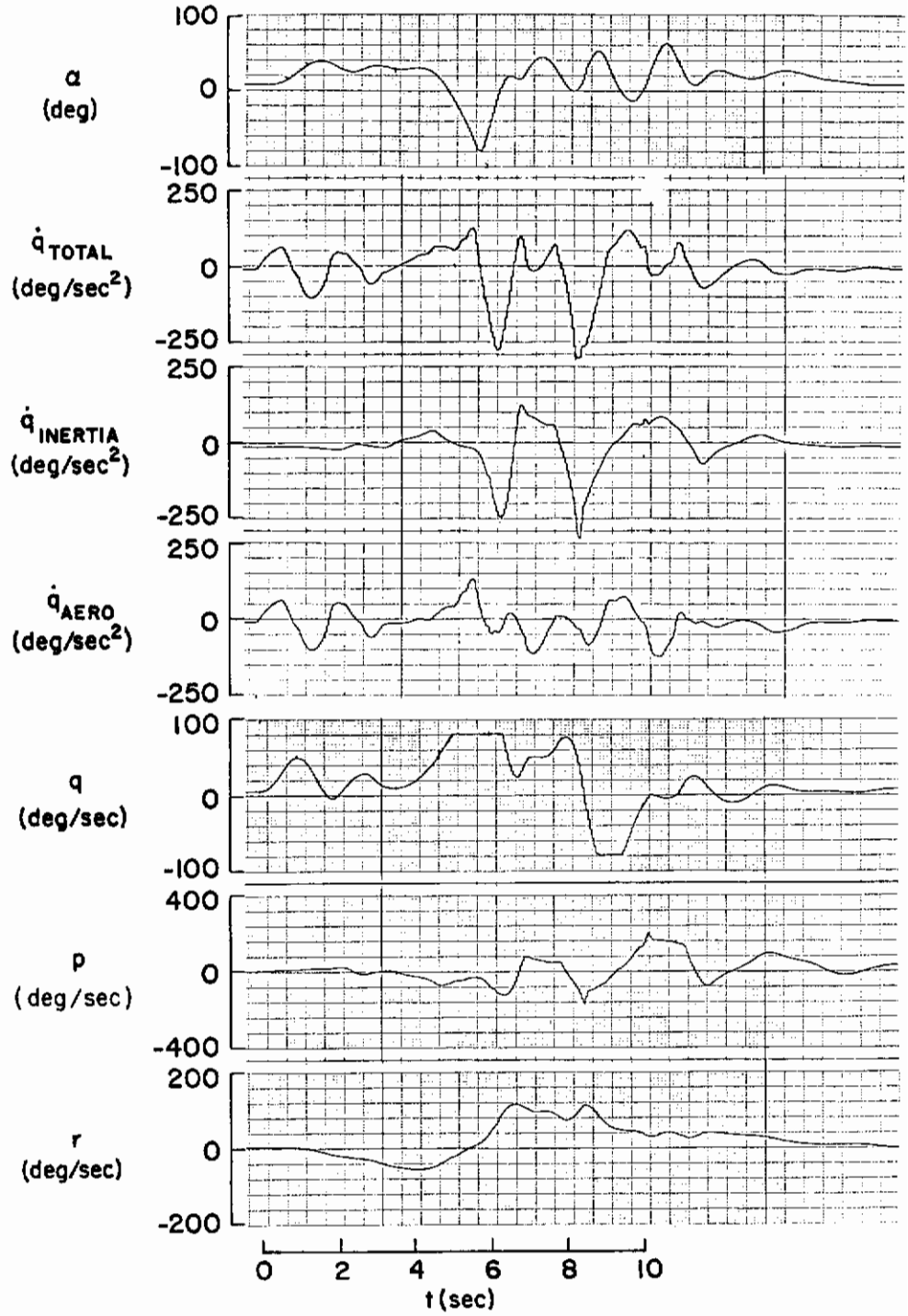

Figure 12. Influence of Inertia Coupling, Configuration D (Piloted Simulation)

The Euler moment equations with the complete inertia terms are:

$$\dot{p} = G\left\{\left[(I_y - I_z)\, I_z - I_{xz}^2\right] r + (I_x - I_y + I_z)\, I_{xz} p\right\} q + GI_z \mathcal{L} + GI_{xz} N$$

$$\dot{q} = \frac{I_z - I_x}{I_y} rp + \frac{I_{xz}}{I_y}\left(r^2 - p^2\right) + \frac{1}{I_y} M$$

$$\dot{r} = G\left\{\left[(I_x - I_y)\, I_x + I_{xz}^2\right] p + (I_y - I_z - I_x)\, I_{xz} r\right\} q + GI_x N + GI_{xz} \mathcal{L}$$

where $G = 1/(I_x I_z - I_{xz}^2)$; I_x, I_y, I_z, and I_{xz} are the moments and product of inertia with respect to the body axes; and $\mathcal{L}$, M, and N are moments about the body axes due to aerodynamics and aircraft thrust. If the relatively small I_{xz} contribution is ignored (as was the case in Ref. 2), the equations reduce to:

$$\dot{p} = \frac{I_y - I_z}{I_x} rq + \frac{\bar{q}Sb}{I_x} C_\ell$$

$$\dot{q} = \frac{I_z - I_x}{I_y} rp + \frac{\bar{q}S\bar{c}}{I_y} C_m$$

$$\dot{r} = \frac{I_x - I_y}{I_z} pq + \frac{\bar{q}Sb}{I_z} C_n$$

Since the inertia coefficient of the $\dot{q}$ equation is positive, then positive r and p produce pitch-up moment and increased AOA (as in Figs. 3, 4, 8, and 9) while positive r and negative p produce pitch-down moment and decreased AOA (as in Figs. 11 and 12).

Reference 2 indicates that the departure criterion was influenced only slightly by inertia changes, despite the fact that the peak AOA ($\hat{\alpha}$) during control input was used to define departure. In that investigation only the cross-coupling terms $(I_z - I_x)$ and $(I_x - I_y)$ in the equations of motion were varied to approximate airframes differing in mass distribution into or away from the fuselage (change in I_x). It was assumed that $I_y - I_z$ did not change. The individual inertias (I_x, I_y, and I_z) were not varied; in particular, changing I_x would have influenced the inertia term of the roll acceleration

equation as well as all aerodynamic acceleration and damping characteristics. Thus, the balance between inertia coupling and aerodynamic counter-acceleration or restoring moments was altered only in the $\dot{q}$ and $\dot{r}$ equations.

It will be recalled that the inertias used in this and the Ref. 2 investigations are nearly identical, and the aerodynamic variations are quite similar. All of the simulation traces show inertial coupling to predominate during large, sustained yaw-rate excursions. Thus the principal coupling is into $\dot{q}$ via rp and $\dot{p}$ via rq. It seems apparent that if the individual inertias I_X or I_Y were to be changed, there would be a corresponding change in the roll and yaw accelerations achievable due to control surface deflections and static aerodynamic instabilities. Hence there would be a change in the pitch inertia-coupling drivers. By analogy, the same is true for roll acceleration.

Based on the vehicle motions observed in this simulation investigation, the peak AOA excursions obtained and the propensity to PSG were significantly influenced by inertial coupling. Again noting the similarity between the vehicle configurations used in this and the Ref. 2 investigations, it appears that broad applicability of the Ref. 2 criterion might be limited by inertia differences.

SECTION VI

SUMMARY AND CONCLUSIONS

A piloted simulation assessment of the Ref. 2 full-control-deflection departure maneuver was performed as a part of an investigation of high AOA maneuver limiting factors. The basic purposes were to:

- Compare simulation and computation results
- Test the Bihrle departure criterion using independently derived (but similar) vehicle configurations
- Obtain pilot assessment of the maneuver's value

A comparison of the Bihrle and Weissman departure criteria was also made, since the latter was a factor in selecting the aerodynamic configurations used.

Comparison of the piloted inputs vis-a-vis computer-programmed inputs shows widely differing results. The piloted simulation maneuvers were much more prone to violent departure and PSG. Responses to control surface deflections differed widely due to nonideal trim conditions prior to control inputs. It was difficult for pilots to achieve pure (non cross-coupled), precisely-timed control inputs. The vehicle responses and departure characteristics were quite sensitive to all of these nonideal conditions.

Results were in reasonable agreement with the Bihrle departure criterion, since that had forecast departure for three configurations and marginal susceptibility for the fourth. All four produced departure and PSG in the piloted simulation. However, results were not consistent with either the peak AOA departure definition used in Ref. 2 or with the pilot assessment of the aircraft motions.

Overall, predicted versus actual departure tendencies and characteristics were more consistent between the Weissman criterion and pilot assessments during closed-loop tracking tasks. The pilots also questioned the usefulness and practicality of the open-loop full-control-deflection maneuver.

Post-nose-slice departure motions obtained in both the piloted and unpiloted simulations were dominated by inertia-coupled PSG which then influenced the AOA excursions obtained. The vehicle motions observed indicate the Bihrle criteria boundaries might be valid only for aircraft having inertia values comparable to those used in this and the Ref. 2 studies. It is recommended that this be investigated further.

REFERENCES

1. Johnston, D. E., D. G. Mitchell, and T. T. Myers, Investigation of High-Angle-of-Attack Maneuver-Limiting Factors, Part I, Analysis and Simulation, AFWAL-TR-80-3141, Dec. 1980.

2. Bihrle, W., Jr., and B. Barnhart, Design Charts and Boundaries for Identifying Departure Resistant Fighter Configurations, NACD-76154-30, July 1978.

3. Weissman, R., "Status of Design Criteria for Predicting Departure Characteristics and Spin Susceptibility," J. Aircraft, Vol. 12, No. 12, Dec. 1975.

4. "Military Specification of Stall/Post Stall/Spin Flight Test Demonstration Requirements for Airplanes," MIL-S-83691A, Apr. 1972.

5. Moul, M. R., and S. W. Paulson, Dynamic Lateral Behavior of High Performance Aircraft, NACA RM No. L58E16, Aug. 1958.

6. Mitchell, D. G., T. T. Myers, G. L. Teper, and D. E. Johnston, Investigation of High-Angle-of-Attack Maneuver-Limiting Factors, Part III: Appendices — Aerodynamic Models, AFWAL-TR-80-3141, Dec. 1980.

7. Sisk, T. R., A Preliminary Assessment of the Transonic Maneuvering Characteristics of Two Advanced Technology Fighter Aircraft, NASA TM X-3439, Sept. 1976.

8. Twisdale, T., Tracking Task Maneuvers for Handling Qualities Evaluation, AFFTC TD75-1, May 1975.

*U.S.Government Printing Office: 1981 — 757-002/604